Journal of Materials Chemistry B

Accepted Manuscript

ROYAL SOCIETY OF CHEMISTRY

www.rsc.org/materialsB

A simple material model to generate epidermal and dermal layers in vitro for skin regeneration

Ching-Ting Tsao[a], Matthew Leung[a], Julia Yu-Fong Chang[b], Miqin Zhang[*a]

[a]Department of Materials Science and Engineering, University of Washington, Seattle, WA 98195, USA.

[b]Department of Oral & Maxillofacial Surgery, University of Washington, Seattle, WA 98195, USA.

Corresponding Author:

Miqin Zhang, Department of Materials Science and Engineering, University of Washington, 302L Roberts Hall, Box 352120, Seattle, WA 98195, USA.

Tel: 1-206-616-9356; Fax: 1-206-543-3100; Email: mzhang@u.washington.edu.

17 TOC

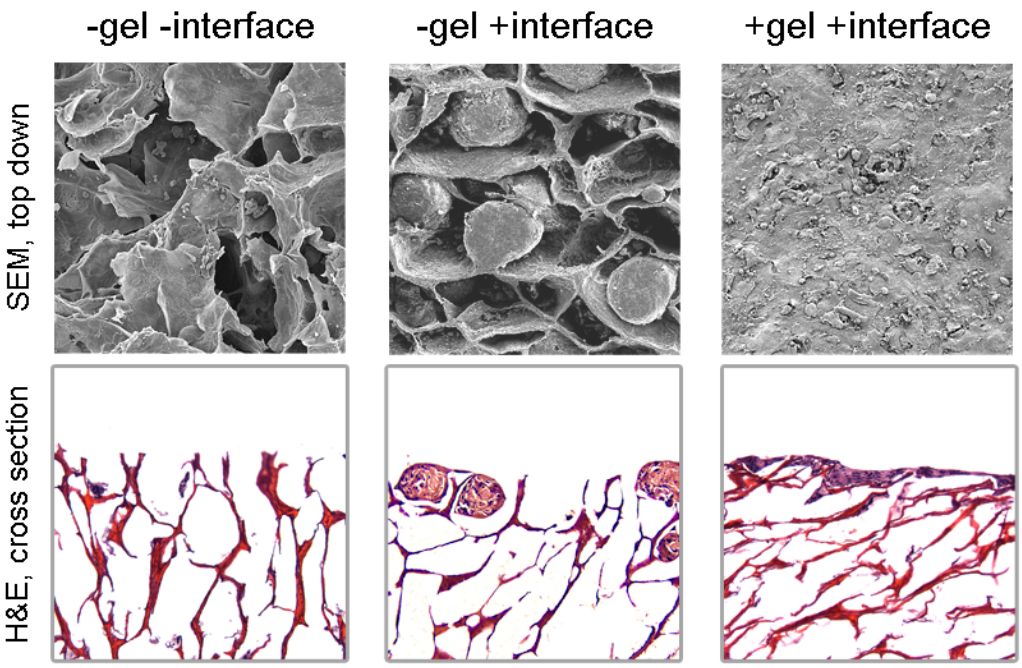

18

19 A porous composite scaffold permeated with chitosan-poly(ethylene glycol) gel, which mimics

20 the bi-layered micro-environment of skin, promotes keratinocyte proliferation and maturation.

21

Abstract

There is an urgent need for a rationally-designed, cellularized skin graft capable of reproducing the micro-environmental cues necessary to promote skin healing and regeneration. To address this need, we developed a composite scaffold, namely, CA/C-PEG, composing of a porous chitosan-alginate (CA) structure impregnated with a thermally reversible chitosan-poly(ethylene glycol) (C-PEG) gel to incorporate skin cells as a bi-layered skin equivalent. Fibroblasts were encapsulated in C-PEG to simulate the dermal layer while the keratinocytes were seeded on the top of CA/C-PEG composite scaffold to mimic the epidermal layer. The CA scaffold provided mechanical support for the C-PEG gel and the C-PEG gel physically segregated the keratinocytes from fibroblasts in the construct. Three different tissue culture micro-environments were tested: CA scaffolds without C-PEG cultured in cell culture medium without air-liquid interface (−gel−interface), CA scaffolds impregnated with C-PEG and cultured in cell culture medium without air-liquid interface (+gel−interface), and CA scaffolds impregnated with C-PEG cultured in cell culture medium with air-liquid interface (+gel+interface). We found that the presence of C-PEG increased the cellular proliferation rates of both keratinocytes and fibroblasts, and the air-liquid interface induced keratinocyte maturation. This CA/C-PEG composite scaffold design is able to recapitulate micro-environments relevant to skin tissue engineering, and may be a useful tool for future skin tissue engineering applications.

Keywords: chitosan, alginate, PEG, hydrogel, skin, ECM

Introduction

Due to its soft and fragile nature, skin can be easily damaged by traumatic injuries or chronic diseases such as diabetes.[1, 2] Skin defects allow the entry of infectious organisms and cause the loss of water, electrolytes and proteins leading to shock. Damage to the integrity of large portions of the skin may result in disability or death, and its treatment constitutes a major health-care burden worldwide.[3] Allogeneic and xenogenic skin grafts have been proven to be useful temporary skin substitutes, but they have limited availability, and bear a severe risk of infection and disease transmission.[4, 5] Autologous skin grafts are the current gold standard treatment for full-thickness skin injuries, but the availability of healthy donor skin is limited, and its collection may result in an additional donor site trauma.[6] The lack of suitable treatments prompts an urgent need for tissue-engineered skin grafts.

One primary hurdle to the development of a successful engineered skin graft is the challenge in replicating the micro-environment present in native skin in which skin cells can grow into bilayer structure to promote dermal-epidermal interactions and form functional skin tissue.[7, 8] Adult skin consists of two layers: a stratified-superficial epidermis and an underlying dermis.[1, 9] The epidermis is comprised of a mixed population of basal keratinocytes with long-term proliferative ability, and a population of committed keratinocytes with limited proliferative ability which form the outer barrier layer.[10] Thus, an effective substitute for the

epidermal matrix must allow keratinocytes to organize vertically and facilitate high density, close packed organization to simulate the native epidermis. The underlying dermis layer is a vascularized bed of connective tissue, which is essential for proper epithelialization.[1] The main component of the dermal extracellular matrix (ECM) is collagen, which is the source of the skin's elasticity, resilience, and mechanical integrity.[11] The fibroblasts in the dermal layer are responsible for the secretion of collagen and maintenance of the dermis.[12, 13] Thus, an engineered skin graft should closely mimic the native bi-layered structure in order to reproduce the numerous physiological functions of human skin.

Currently, a number of cellularized epidermal-dermal skin substitutes developed to mimic the structure of native skin are available for clinical use[14] However, none of these is fully satisfactory and each has limitations. For example, Alloderm® uses acellular dermis substitute to integrate skin cells (keratinocytes, fibroblasts, or both) to generate cellularized, bi-layered skin equivalents.[5] However, poor ingrowth of dermal fibroblasts was observed due to the dense structure of collagen fibrils in Alloderm®, rendering it an unsatisfactory skin graft.[5] Apligraf® is another cellularized skin graft seeded with human foreskin-derived neonatal epidermal keratinocytes and human foreskin-derived neonatal fibroblasts in a bovine type I collagen matrix.[15] Though this construct demonstrated excellent delineation of epidermal and dermal layers, the transplanted skin cells have been found to be viable for just 4 weeks post

transplantation.[16] OrCel® is a bi-layered cellularized product using porous collagen sponge with one side coated with collagen gel. Dermal fibroblasts are cultured within the porous collagen sponge and keratinocytes are seeded on the gel-coated side to prevent the ingrowth of keratinocytes.[17] Though accelerated healing rate and reduced scar formation are achieved with this graft compared with conventional therapy with Biobrane-L synthetic wound dressing,[17] there are no clinical data showing that this graft can replace native skin allograft.[8] Additionally, the collagen-based scaffolds exhibit low stability, low mechanical strength, wound contraction, and poor integration with host tissue.[8, 18] Synthetic polymer based sponge scaffolds were developed to increase the biostability and mechanical strength but the tissue repair is usually accompanied by low healing rate and fibrotic reactions that result in scar formation.[8, 19] Thus alternative material compositions and organizations are needed to address the current limitations of tissue engineered skin grafts.

In this study, we developed a natural polymer-based skin engineering material by permeating a poly(ethylene glycol)-g-chitosan (C-PEG) hydrogel into a three-dimensional, porous chitosan-alginate (CA) scaffold yielding the favorable combination of mechanical and biochemical cues that serve well as an appropriate bi-layered micro-environment to support dermal fibroblasts and the overlaying keratinocytes. Both chitosan and alginate are natural polymers and have the proxy structure of glycosaminoglycans (GAGs),[20] a major component of

the native extracellular matrix (ECM).[21] We have previously shown that 3D porous CA complex scaffolds have high mechanical strength as a result of the ionic bonding of the amine group of chitosan with the carboxyl group of alginate while providing an excellent environment for the generation of tissue engineered cartilage and bone and stem cell renewal.[22-24] Unlike other natural polymers derived from costly mammalian proteins, chitosan and alginate have unlimited sources and evoke minimal foreign body response or fibrous encapsulation[25-28] Poly(ethylene glycol) (PEG) is a neutral, water-soluble, and non-toxic polymer approved by the Food and Drug Administration (FDA) for internal consumption and injection in a variety of foods, cosmetics, personal care products, pharmaceuticals, and biomedical applications.[29] C-PEG was proven to be an injectable and thermally reversible gelling material, which is a liquid at 0°C or below and forms a stable gel at higher temperatures including the body temperature.[30, 31] Cells can be readily released from the thermal reversible gels for subsequent analysis by cooling it.

Dermal fibroblasts were dispersed and cultured within the C-PEG gel that was infused into the porous structure of the CA scaffold. Keratinocytes were seeded on the top of CA/C-PEG scaffold and exposed to an air-liquid interface to promote maturation of the stratified epidermal layer and support maintenance of the fibroblasts. The *in situ* gelation of C-PEG within the pores of the CA scaffold was achieved by increasing the temperature of the gel to the physiological temperature. Cell proliferation, morphology, histology, and gene transcription of cells cultured

CA/C-PEG composite scaffold at different microenvironmental conditions were investigated to evaluate the effectiveness of the CA/C-PEG scaffold for skin regeneration.

Results

Cell proliferation

Cell proliferations of HaCat and hFF were evaluated by cell sorting using FACS to assess cellular compatibility of the composite scaffolds to the HaCat and hFF. Fig. 2 shows the proliferation of HaCaT and hFF cells cultured in 3 microenvironments over 2 weeks. The numbers of both HaCaT and hFF cells increased over time in all 3 conditions. Greater populations of HaCaT and hFF cells were observed in both +gel−interface and +gel+ interface conditions than in the −gel−interface condition. Notably, the numbers of HaCaT and hFF cells were higher in +gel−interface condition than in +gel+interface condition throughout the 2 weeks of culture period.

Cell morphology and interaction with scaffolds

SEM was performed to examine the interaction between cells and the microenvironment via a top-down view. The morphologies of HaCaT and hFF cells after 2 weeks of culture were shown in Fig. 3. In the −gel−interface condition, HaCaT cells were found to unevenly disperse

as minute colonies across the scaffold (Fig. 3a), and showed reduced and limited adhesion with the CA scaffold (Fig. 3d). In the +gel−interface condition, the HaCaT cells were observed to aggregate, forming stacked cell colonies that filled CA scaffold pores and attached firmly to and dispersed uniformly across the scaffold (Fig. 3b). The individual colonies formed a discontinuous layer across the construct surface, and the colony of cells at a high magnification (Fig. 3e) clearly showed that cells adhered to scaffolds well. In the +gel+interface condition, the HaCaT cells were shown to form a dense layer over the scaffold (Fig. 3c) and superimpose on top of each other forming dense multi-layered aggregates (Fig. 3f). On the other hand, there is no significant difference in cellular distribution pattern of hFF cells among the 3 culture conditions after 2 weeks, but a significant difference in the cellular morphology. hFF cells showed a spherical morphology in −gel−interface condition (Fig. 3g), a typical spindle morphology in both +gel−interface (Fig. 3h) and +gel+interface conditions (Fig. 3i).

Histology was performed to evaluate the cellular distribution and organization in the microenvironment via a cross-sectional view. Fig. 4 shows the hematoxylin and eosin (H&E) stained HaCaT and hFF cells after 2 weeks of culture. HaCaT cells in the −gel−interface condition were observed to have fallen into the porous compartments of CA scaffold and formed tiny colonies (Fig. 4a and 4d), which is consistent with the SEM finding. On the other hand, HaCaT cells in the +gel−interface condition were found to form a larger, multi-layered

colonies but discontinuous layers across the top of the construct (Fig. 4b and 4e). In contrast to the other two conditions, HaCaT cells in +gel+interface condition were observed to grow and organize into a continuous stratified epithelial layer with slightly cuboidal in the basal layer and flattened in the superficial layers (Fig. 4c and 4f). Similar to the result revealed in SEM analysis, there was no significant difference in cellular distribution pattern of hFF among the three conditions.

Fluorescent images were taken to characterize the cellular distribution pattern of both keratinocytes and fibroblasts in the culture microenvironment via a cross-section view. Fig. 5 shows the fluorescent image of HaCaT (red, RFP) and hFF (green, GFP) cells after 2 weeks of culture. HaCaT cells in −gel−interface condition exhibited as small colonies, scattering unevenly in the porous CA scaffold (Fig. 5a) while those in +gel−interface condition formed discontinuous cell clusters (Fig. 5b). HaCaT cells in the +gel+interface condition formed a continuous layer with 1–3 cell layers in thickness connecting between larger cell clusters (Fig. 5c). While there was no significant difference in cellular distribution pattern for hFF, the cellular morphology of hFF cells varied between conditions. hFF cells exhibited similar morphology in −gel−interface (Fig. 5d), +gel−interface (Fig. 5e) and +gel+interface (Fig. 5f) conditions. The results from the fluorescence images corroborate well those from SEM and histological analyses.

168

169 **mRNA analysis of cellular behavior**

170 To determine gene transcription profiles of HaCaT and hFF cells co-cultured in different
171 microenvironments, real-time RT-PCR was performed on HaCaT (RFP) and hFF (GFP) cells that
172 were sorted by FACS. RNA transcriptions of Collagen I, Collagen III, fibronectin and vimentin
173 by fibroblasts, and keratin 5 and keratin 10 by keratinocytes were evaluated due to their key roles
174 in skin wound healing.[32-36] Keratin 5 and keratin 10 expressions represent the basal cell layer and
175 differentiated spinous cell layer, respectively.[37-40] During the migration of the keratinocytes from
176 stratum basale to the stratum corneum, they express various keratins which specifically indicate
177 their differentiation state.[41] The keratinocytes of the basal layer are highly proliferating and
178 expressing keratin 5.[42] As they migrate into the superficial layer, they become increasingly
179 differentiated. Cells of the uppermost of keratinizing epithelia express keratin 10.[42]

180 The keratinocyte gene transcription changes in response to microenvironments of constructs
181 were shown in Fig. 6. The highest expression of keratin 5 was found in +gel−interface
182 condition, indicating the existence of more less-differentiated basal cells in this condition. In
183 contrast, the highest expression of keratin 10 was observed in +gel+interface condition,
184 indicating the presence of a population of more differentiated cells.

185 On the other hand, Collagen I, the predominant collagen type in human skin,[43] is produced

mainly by fibroblasts,[44] and is important for cell adhesion and migration within connective tissues.[45] In comparison, collagen III is an ECM protein observed to be synthesized during the initial stages of wound healing.[46] Fibronectin plays many roles in wound healing and is produced locally by fibroblasts in regions where epidermal cell migration occurs.[47] Vimentin constitutes a major portion of the cytoskeleton, plays an important role in supporting organelle organization and contributes to the plasma membrane fusion machinery in fibroblasts.[48] Furthermore, fibronectin and vimentin have been reported to be involved in fibroblast adhesion.[45] The effect of microenvironmental conditions of the dermal layer on the gene transcription changes was shown in Fig. 7. Generally, the signal of collagen I, collagen III, fibronectin and vimentin of hFF cells showed no statistical difference between －gel－interface and ＋gel－interface conditions, but the highest expression among the 3 culture microenvironments was observed in the ＋gel＋ interface condition.

Discussion

In this work, a thermally reversible chitosan-g-poly(ethylene glycol) hydrogel (C-PEG) reinforced with a porous chitosan-alginate (CA) scaffold was developed as skin equivalent. With its rationally designed structure (Fig. 1c-d), this composite material was used to mimic the bi-layered structure of native skin.

The cellular microenvironment, comprised of features including soluble factors, extracellular matrix (ECM), and cell-cell interactions can dictate cell behavior *in vivo*.[7] Therefore, improved control over these interactions can better direct the development and function of engineered tissues. In this study, with constantly increasing cell number over the culturing period of 2 weeks, both CA scaffold and C-PEG were shown to have good biocompatibility with HaCaT and hFF cells (Fig. 2). Furthermore, the cellular population in both +gel−interface and +gel +interface conditions were greater than those in −gel−interface condition. This result suggests that the C-PEG provided a suitable microenvironment for HaCat and hFF cell interactions, which promoted cell proliferation. This might be due to the fact that keratinocyte signaling via soluble factors stimulates fibroblasts to synthesize growth factors, which in turn would stimulate keratinocyte proliferation in a paracrine manner.[7,36,49] The decreased cellular proliferation for both cell types was observed in +gel+interface as compared to +gel− interface. This corroborated the results from other studies that the activities of both fibroblasts and keratinocytes are down-regulated in wound healing compared with those in normal skin regeneration.[36,49,50] Furthermore, the distribution pattern of HaCaT cells indicated that −gel− interface condition (Fig. 4a, 4d and 5a) was unable to provide a suitable environment for HaCaT cells to form a continuous barrier in 2 weeks. In contrast, the C-PEG with CA composite scaffold was able to provide a suitable microenvironment for proper cell spreading and adhesion in both

+gel−interface (Fig. 4b, 4e and 5b) and +gel+interface conditions (Fig. 4c, 4f, and 5c). Notably, the cellular population was larger in +gel−interface condition than in +gel+interface condition (Fig. 2). The effect of air-liquid interface on differentiation has been known in organ-cultured keratinocytes.[10, 51] Accordingly, HaCaT cells cultured in +gel+interface were found to show a continuous striated cell layer as in native skin (Fig. 4b, 4e and 5b), rather than the discrete pattern observed in +gel−interface (Fig. 4c, 4f, and 5c). This suggests that the air-liquid-interface may significantly contribute to cell differentiation rather than the cell proliferation while+gel−interface promote proliferation of individual cells rather than the cell differentiation and maturation.

Our real-time PCR results showed that the existence of basal cell characteristics in +gel− interface condition and the existence of differentiated spinous cell characteristics in +gel+ interface (Fig. 6). In the +gel+interface culture condition, expression of keratin 10, a mRNA marker of keratinocyte maturation were significantly upregulated compared to other culture conditions, with a corresponding decrease in the expression of keratin 5, a marker of basal keratinocytes. This relationship between expression of genes associated with maturing keratinocytes and culture conditions suggested that the air-liquid interface may be a major factor in promoting keratinocyte differentiation. In contrast, while Collagen I is the predominant collagen in normal human skin and exceeds Collagen III by a ratio of 4:1, this ratio decreases to

2:1 in wound healing, due to an early increase in the deposition of Collagen III.[52] The hFF gene expression pattern observed in this study suggests that the culture microenvironment of the + gel + interface condition elicited a cellular response comparable to what would be expected from an initial wound healing response *in vivo*. Early deposition of collagen III at the wound site appears as a crucial step for evaluation of the non-scarring healing process. As Collagen III synthesis is found to be upregulated by dermal fibroblasts in + gel + interface condition, it is possible that the microenvironment of + gel + interface condition may contribute to a non-scarring wound healing process.[52]

Other studies of cellularized tissue engineered skin equivalents had difficulty in separation of epithelia keratinocytes from dermal fibroblasts for further investigation.[7,41,53] Both keratinocytes and fibroblasts could be readily released from our materials developed herein and sorted by the FACS. Significantly, our results indicated that the unique microenvironment created by C-PEG gel and CA scaffold along with air-liquid interface is able to direct cell behavior towards a desirable proliferative response and stimulate the expression of relevant *in vivo* wound healing markers and cellular activity in an *in vitro* environment.

Conclusions

In this study, we have demonstrated the fabrication and *in vitro* performance of a novel C-PEG gel and CA composite scaffold that can accommodate fibroblasts and karatinocytes to

form a bi-layered tissue engineered skin equivalent. The composite scaffold segregated the two cell types into a three-dimensional dermal layer and a flat epidermal layer with air-liquid-interface. In these unique microenvironments, both cell types expressed their characteristic mRNA markers. Gene transcription expression confirmed that the bi-layered construct provided a microenvironment that stimulated an initial wound healing response with enhanced collagen secretion in the dermal fibroblast compartment. The epidermal layer in the composite scaffold contributed expression of gene markers for differentiation, along with histological features of keratinocyte differentiation into stratified layers. Furthermore, the bi-phasic scaffold design may be applicable for the generation of other complex tissues composed of two tissue types in tissue engineering or developmental biology contexts.

Experimental

Materials

All chemicals were purchased from Sigma-Aldrich (St. Louis, MO) unless otherwise specified. Chitosan (85% de-acetylated, MW = medium), alginate (alginic acid from brown seaweed, Mw = 80,000–120,000 Da) and methoxy-poly(ethylene glycol) (PEG, Mw = 2,000 Da) were used as received.

Dulbecco's Modified Eagle Medium (DMEM), antibiotic-antimycotic (AA), Dulbecco's

phosphate buffered saline (D-PBS), Trypsin-EDTA, Lipofectamine® 2000 reagent, and haematoxylin-eosin (H&E) were purchased from Invitrogen (Carlsbad, CA). Plasmid Mega Kit, QIAshredder columns, and SYBR Green PCR Master mix were purchased from Qiagen (Valencia, CA, USA). The fetal bovine serum (FBS) was procured from Atlanta Biologicals (Lawrenceville, GA).

Human foreskin fibroblasts (hFF) were purchased from American Type Culture Collection (ATCC, Manassas, VA) and Keratinocytes (HaCaT) were purchased from Cell Lines Service (Germany). The cells were maintained according to the instructions provided by each manufacturer and fully supplemented in DMEM with 10% FBS and 1% AA at 37°C and 5% CO_2 in a fully humidified incubator.

Scaffold preparation

Chitosan-poly(ethylene glycol) (C-PEG) hydrogel

C-PEG was prepared as previously reported.[54, 55] Briefly, PEG-aldehyde was prepared utilizing the following procedure to oxidatize PEG with DMSO/acetic anhydride. First, the PEG was completely dissolved in anhydrous DMSO/chloroform (90/10, v/v), followed by the addition of acetic anhydride to the mixture under a nitrogen atmosphere until the molar ratio of acetic anhydride to PEG was 12. The mixture was then stirred for 12 hr at room temperature under a

nitrogen atmosphere and precipitated using excess diethyl ether. With chloroform, the precipitate was dissolved and then once again precipitated with diethyl ether. After vacuum drying, a white PEG-aldehyde powder was obtained. Utilizing a Schiff base formation, C-PEG was prepared by the alkylation of chitosan using the PEG-aldehyde. To do this, chitosan and PEG-aldehyde with a weight ratio of 0.3 were added into a mixture of acetic acid/methanol (80/100, v/v) to obtain a solution of pH 6. Aqueous cyanoborohydride ($NaCNBH_3$) solution was then added drop-wise into the mixture of chitosan and PEG-aldehyde in a molar ratio of 0.02/0.3 to form $NaCNBH_3$/PEG-aldehyde. Twenty hr after the reaction, the resultant mixture was dialyzed using a dialysis membrane (MW 12000–14000 cut off) against DI water and 0.05 M NaOH, and then DI water again until a neutral pH was reached. The solution was subsequently freeze-dried. With excess acetone, residual PEG-aldehyde was removed from the freeze-dried samples resulting in C-PEG powder. The C-PEG powder was sterilized with EtO gas prior to being re-constituted in cell culture media. Finally, a 2% C-PEG hydrogel solution was prepared using DMEM supplemented with 10% FBS.

Chitosan–alginate (CA) scaffolds

The CA scaffold was prepared as previously reported.[22, 23, 56] First, two separate solutions were prepared: a 4% chitosan in 1% acetic acid aqueous solution, and a 4% alginate solution in

DI water. The two solutions were then blended using a mixer (ARM-300, Thinky) at 2000 rpm for several min to obtain a homogenous mixture. The solution was then cast into each individual well in a 24-well plate, maintained at –20°C for 24 hr, and lyophilized to form a porous CA scaffold. The CA scaffold was then cross-linked by 0.2 M $CaCl_2$ for 10 min, and washed with DI water. The CA scaffold was sanitized using 70% ethanol, and was repeatedly washed with PBS to remove residual ethanol before cell culture.

Plasmid DNA

Plasmids containing a CMV promoter and green fluorescence protein / red fluorescence reporter (pGFP-N2, 4.7 kb/pRFP–N2, 4.7kb) were obtained from BD Biosciences Clontech (Palo Alto, CA, USA). pGFP-N2/pRFP–N2 plasmid DNA were amplified in bacteria and extracted using a Plasmid Mega Kit. The recovered plasmids were stored at 4°C in sterilized DI water. The purified plasmids were analyzed by gel electrophoresis, while their concentration was measured by UV absorption at 260 nm (V-530, Jasco, Tokyo, Japan).

Cell transfection

Prior to transfection, an appropriated amount of HaCaT and hFF cells were separately seeded into a 6-well plate containing antibiotic-free culture media. 24 hr after plating, HaCaT

and hFF cells were transfected with pRFP–N2 and pGFP-N2, respectively using Lipofectamine® 2000 Reagent following the manufacturer's instructions. 48 hr after transfection, the cells were washed with PBS and supplied with fresh medium, and then selected with G418-containing media (500 μg/mL). 2 weeks after selection, the cells were sorted by fluorescence activated cell sorting (Aria III Sorter; Vantage SE). For simplicity, HaCaT+RFP is abbreviated as HaCaT, and hFF+GFP as hFF hereafter.

Characterization

Cell seeding and culturing

The fibroblast (hFF) and karatinocytes (HaCaT) were cultured on the three microenvironments including (1) CA scaffold without gel in cell culture medium without air-liquid interface (−gel−interface), (2) CA scaffold permeated with C-PEG (+gel− interface) in cell culture medium without air-liquid interface, and (3) CA scaffold permeated with C-PEG cultured at the air-liquid interface (+gel+interface). The schematic representations of the three culture conditions were illustrated in Fig. 1a, 1b, and 1c, respectively. Specifically, for the culture condition of −gel−interface, 10^5 hFF cells were seeded directly into CA scaffold. 2 hr after the seeding of hFF, 5×10^5 HaCaT cells were seeded onto CA scaffold, followed by addition 500 μL of DMEM. For the culture condition of +gel−interface, 10^5 hFF

cells were suspended in 200 μL of 2% C-PEG at 4°C, and subsequently poured onto a CA scaffold. The *in situ* gelation of C-PEG was achieved by maintaining construct at 37°C for 2 hr. After the gelation, 5×10^5 HaCaT cells were seeded on the top of the C-PEG layer, followed by addition of 300 μL of DMEM. The medium changes were performed every other day. For the culture condition of +gel+interface, all the conditions were the same as +gel−interface except the CA scaffold sitting in a Transwell insert (polycarbonate membrane, 0.4 μm, Corning, Lowell, MA). To create the air-liquid-interface, 500 μL of DMEM was added to the Transwell, which was not higher than the surface of seeded HaCat cells. Fig. 1d shows the *in situ* gelation of hFF/C-PEG gel mixture within CA scaffold. Fig. 1e shows +gel+interface were overlaid by HaCaT cells after 2 weeks of culture in the Transwell insert.

Cell proliferation

For cell number quantification, the scaffold was degraded to detach the seeded detach the seeded HaCaT+RFP and hFF+GFP cells at specific time interval of 5, 10, and 14 d. Specifically, the scaffold was immersed in the solution of 30 mM $NaHCO_3$ in 5 mM HEPES for 10 min at 37°C and the solution of 10 mM EDTA in 20 mM HEPES was then added for another 10 min immersion at 37ºC. The solution was filtered through a 70 micron filter to eliminate the scaffold debris. The filtered cells were further detached with Trypsin EDTA (Invitrogen) and washed with PBS for 3 times. The cell pellet was re-suspended in 1% FBS in PBS, and were then sorted and

quantified by flow cytometry (BD Aria III Sorter; Becton Dickinson, San Jose, A). Cell sorting was performed using RFP signals (excitation with the 561 nm laser, emission detection at 582/15 nm), and GFP signals (excitation with the 488 nm laser, emission detection at 530/30). Gates were set to exclude necrotic cells and cellular debris and the fluorescence intensity of events within the gated regions was quantified. The resulting sorted cells were re-suspended in fresh media for further analysis (PCR).

Scanning electron microscopy

To conduct SEM analysis, cell-scaffold constructs were removed from culture medium after 2 weeks of culture, rinsed with PBS, and fixed with formalin for 30 min. Once fixed, specimens were rinsed with DI water 3 times, dehydrated with sequential incubations in 70%, 85%, 95% and 100% ethanol for 20 min each, and then critical point CO_2 dried using a Hitachi HCP-2 (Hitachi, Tokyo, Japan). The specimens were sputter-coated with Au/Pd at 18 mA for 40 sec, and imaged by scanning electron microscopy (SEM, JEOL JSM 7000).

Histology

For histological analysis, cell-scaffold constructs were fixed with formalin for 30 min, then dehydrated with sequential incubations in 70%, 85%, 95%, 100% ethanol, and xylene for 1 hr at each step. Samples were embedded into paraffin, cross sectioned into 10-μm-thick sections.

Samples were then stained with hematoxylin and eosin (H&E), and visualized with an optical microscope (Nikon).

Real-time PCR

In each culture condition, cells were first detached from scaffolds, and then the HaCaT and the hFF cells were sorted by fluorescence activated cell sorting (FACS; Vantage SE) for further PCR analysis.

Cells were homogenized by vortexing and passed through the QIAshredder (Qiagen) columns for each RNA separately. The total RNA was isolated using RNeasy with 30 ng of total RNA from a triplicate sample converted to cDNA following the manufacturer's instructions for the QuantiTect Reverse Transcription Kit (Qiagen). SYBR Green PCR Master Mix (BioRad) was used with a primer for template amplification for each of the transcripts examined. Thermocycling was performed at the following conditions: 95°C for 15 min, 45 cycles of denaturation (94°C, 15 sec), annealing (55°C, 30 sec), and extension (72°C, 30 sec). The reaction was monitored in real-time using a CFX96 Real-Time System (BioRad). For relative quantification via the delta-delta Ct method, the ratio of the expression levels in the two samples was calculated using β-actin as a reference transcript for normalization. Samples were assayed in triplicate, and primers used are listed in Table 1.

Statistical analysis

The results were presented as mean values of triplicate samples ± standard deviation. The statistical difference was determined by unpaired, two-tailed Student's *t*-test. Values were considered to be statistically significant at $p < 0.05$ (*).

Acknowledgements

This work is supported in part by NIH grant (NIH/NCI R01CA172455) and Kyocera Professor Endowment to M.Z. We acknowledge the use of resources at the Center for Nanotechnology and Department of Immunology at the University of Washington.

Figures

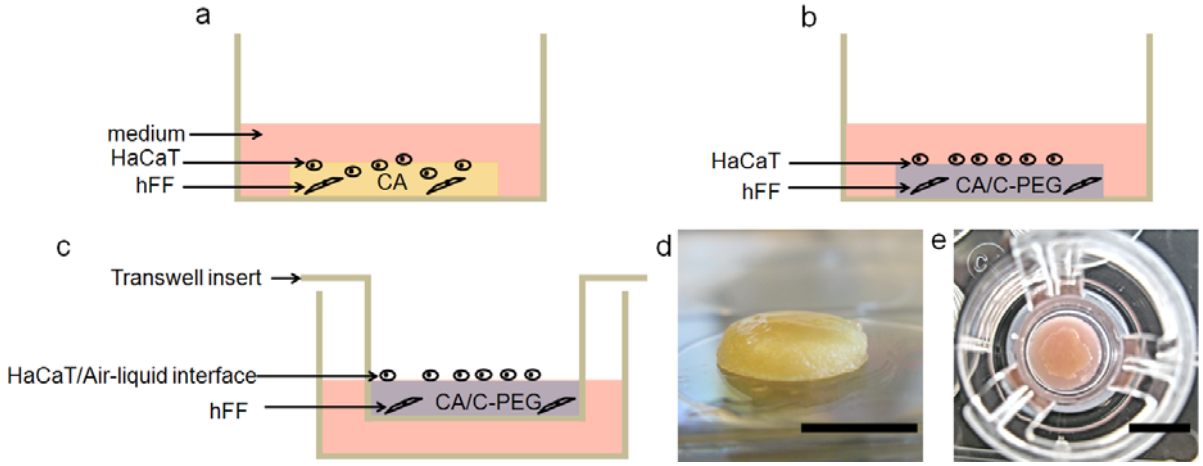

Fig. 1. Schematic illustration of co-culture of HaCaT and hFF cells in (a) CA scaffolds (－gel－ interface, labeled in yellow) (b) CA scaffolds with C-PEG gel (＋gel－interface, labeled in grey),

and (c) CA scaffolds with C-PEG gel and air-liquid interface (+gel+interface, labeled in grey with air-liquid interface created by transwell insert). (d) *in situ* gelation of hFF/C-PEG gel mixture within CA scaffold; this side-view picture emphasizes the C-PEG gel on of the surface of CA scaffold. (e) Top-down view of C-PEG gel overlaid with HaCaT epithelial cells after 2 weeks of culture in the Transwell insert. Both scale bars represent 1 cm.

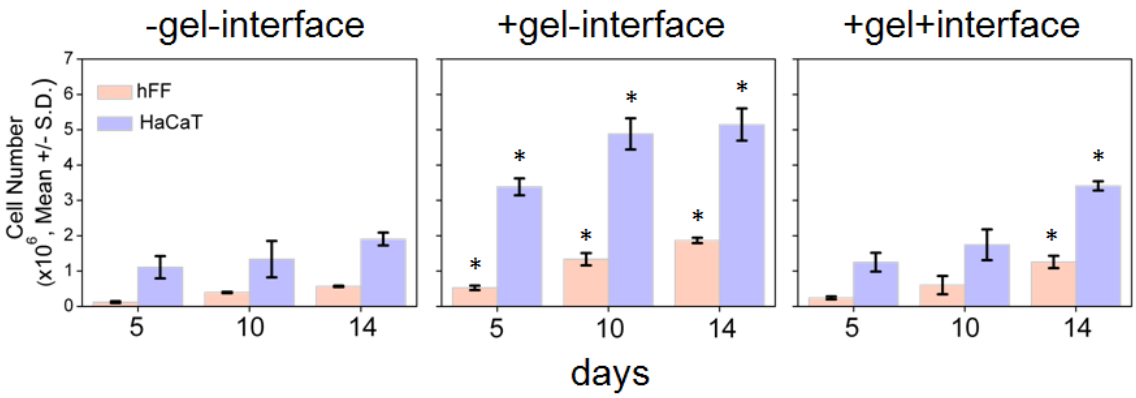

Fig. 2. Proliferation analysis of HaCaT and hFF cells in 3 different microenvironments over 14 days as determined by cell sorting. * indicates a statistical significance in cell numbers of hFF and HaCaT ($p < 0.05$) as compared to respective cells at the −gel−interface condition and at each respective time point.

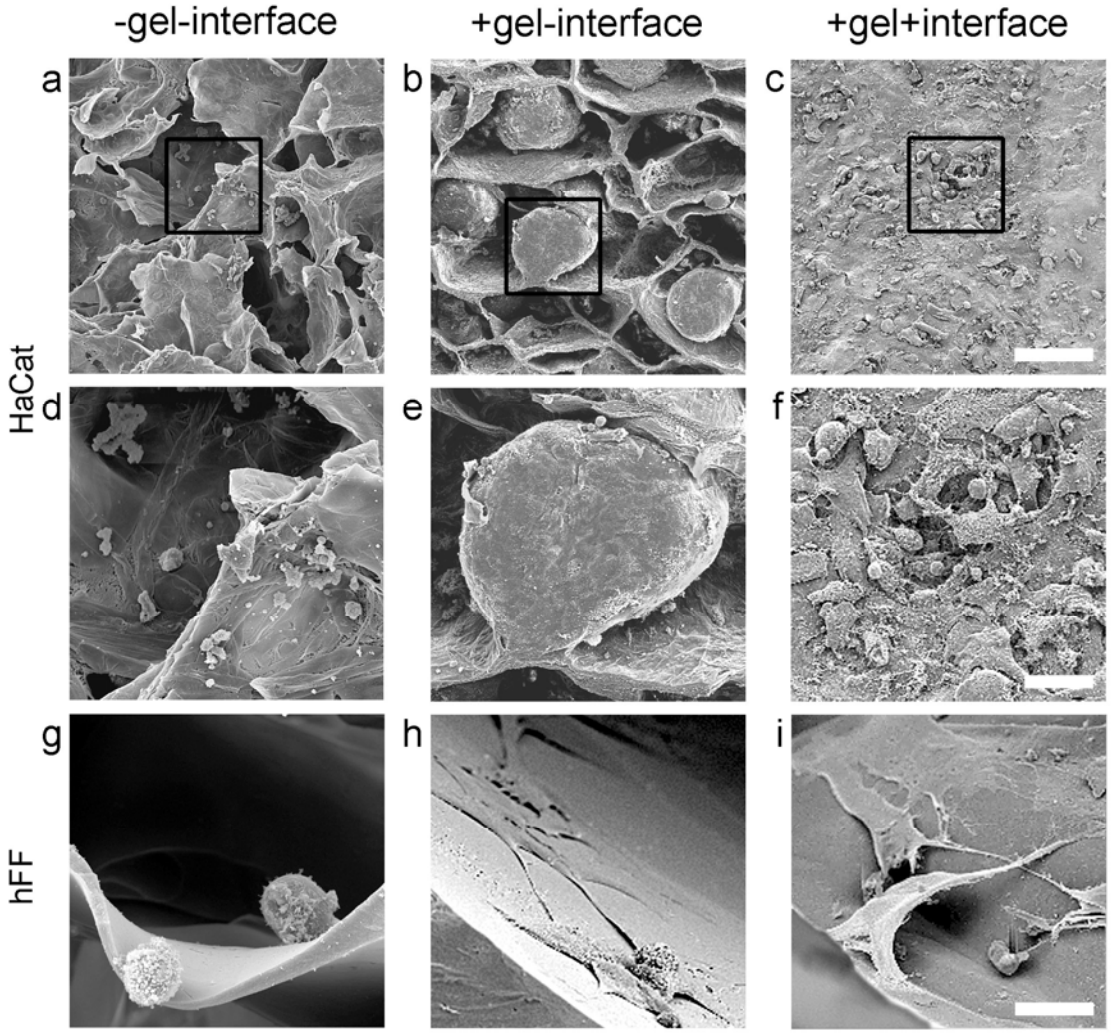

Fig. 3. SEM images of HaCaT/hFF cells cultured in 3 different microenvironments for 2 weeks: －gel－interface (a, d, g), ＋gel－interface (b, e, h), and ＋gel＋interface (c, f, i). For HaCaT cells, the black boxes in low magnification images (a, b, c, scale bar = 100 μm) identify the areas in high magnification images (d, e, f, scale bar = 25 μm). For hFF cells in g, h, i, scale bar = 15 μm.

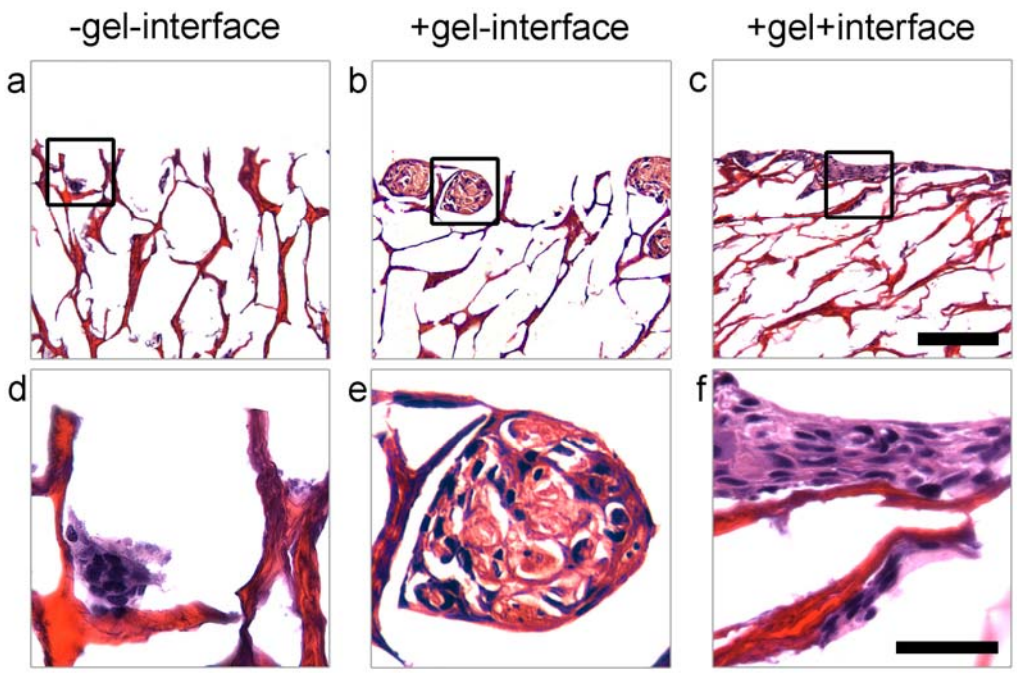

Fig. 4. Histological analysis of HaCaT cells cultured in 3 different microenvironments for 2 weeks: −gel−interface (a, d), +gel−interface (b, e), and +gel+interface (c, f). For HaCaT cells, the black boxes in low magnification images (a, b, c, scale bar = 20 μm) identify the areas in high magnification images (d, e, f, scale bar = 5 μm).

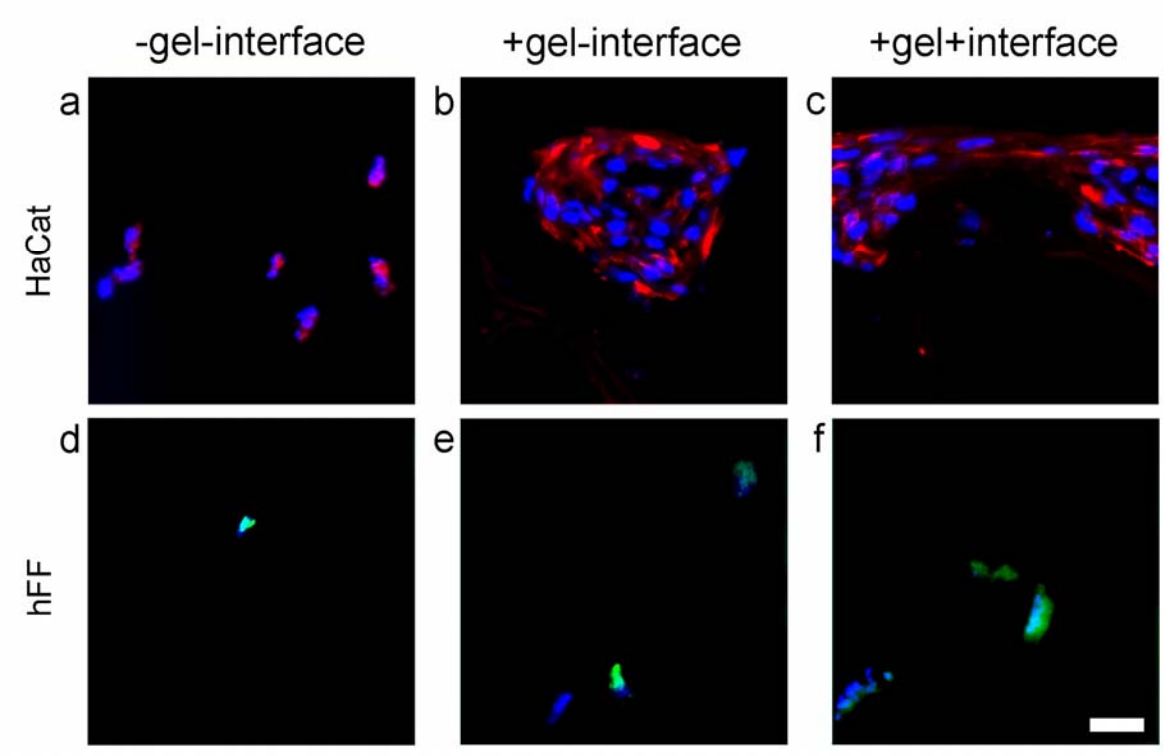

Fig. 5. Fluorescent images of HaCaT/hFF cells cultured in 3 different microenvironments for 2 weeks: −gel−interface (a, d), +gel−interface (b, e), and +gel+interface (c, f). Cellular nuclei are blue, HaCat and hFF cells express red and green fluorescence, respectively. Scale bar = 25 μm.

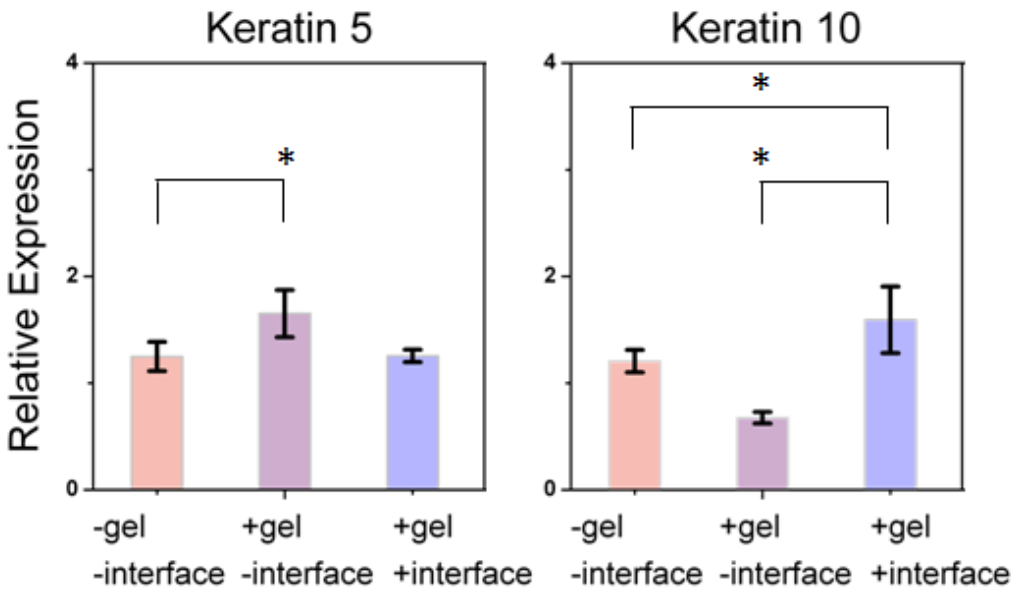

Fig. 6. RNA transcription of Keratin 5, and Keratin 10 by HaCaT cells cultured in 3 different microenvironments for 2 weeks: −gel−interface, +gel−interface, and +gel+interface. Results are normalized to β-actin mRNA. *indicates a statistical significance ($p < 0.05$) of +gel +interface as compared to other conditions.

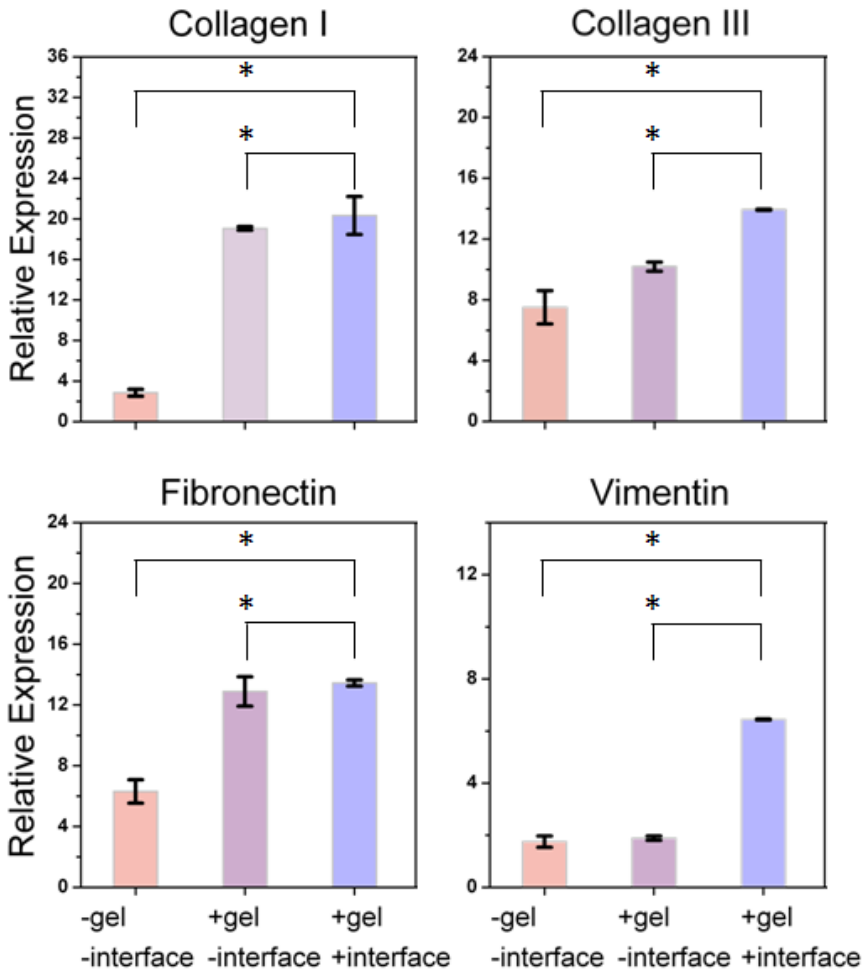

Fig. 7. RNA transcription of Collagen I and III, Fibronectin, and Vimentin expressed by hFF cells cultured in 3 different microenvironments for 2 weeks: −gel−interface, +gel−interface, and +gel+interface. Results are normalized to β-actin mRNA. * indicates a statistical significance ($p < 0.05$) of +gel+interface as compared to other conditions.

501 Table 1: Primer sequences used for real-time PCR analysis.

Gene of Interest		Sequence (5'-3')
β-actin (ACTA2)	*Forward*	TCGCATCAAGGCCCAAGAAA
	Reverse	CAGGATTCCCGTCTTAGTCCC
Keratin 4 (KRT4)	*Forward*	AGGTGCCTTCAGCTCAGTCT
	Reverse	CCAAAGCAGGCACCTTGTCG
Keratin 5 (KRT5)	*Forward*	AACCCACTAGTGCCTGGTTC
	Reverse	AAGGACACACTTGACTGGCG
Keratin 10 (KRT10)	*Forward*	CAGATAGGCCAGCTCTTCAGTCA
	Reverse	GACATCAACGGCCTGCGTA
Keratin 17 (KRT17)	*Forward*	GTCACGCATCTCGTTGAGGA
	Reverse	AGGTGGGTGGTGAGATCAATG
Keratin 19 (KRT19)	*Forward*	TCATATTGGCTTCGCATGTCA
	Reverse	CAGGTCAGTGTGGAGGTGGA
Collagen I (COL1A1)	*Forward*	ACATGTTCAGCTTTGTGGACC
	Reverse	CATGGTACCTGAGGCCGTTC
Collagen III (COL3A1)	*Forward*	ATGTTGTGCAGTTTGCCCAC
	Reverse	TCGTCCGGGTCTACCTGATT
Fibronectin (FN1)	*Forward*	ACAGGAAAGAGATGCGCCAA
	Reverse	GGAAGAGTTTAGCGGGGTCC
Vimentin (VIM)	*Forward*	TCACCTGTGAAGTGGATGCC
	Reverse	GCAGAGAAATCCTGCTCTCCT

502

503

References

1. H. Wendt, A. Hillmer, K. Reimers, J. W. Kuhbier, F. Schafer-Nolte, C. Allmeling, C. Kasper and P. M. Vogt, *PLoS One*, 2011, **6**, e21833.
2. W. T. Seet, M. Manira, K. Khairul Anuar, K. H. Chua, A. W. Ahmad Irfan, M. H. Ng, B. S. Aminuddin and B. H. Ruszymah, *PLoS One*, 2012, **7**, e40978.
3. R. Papini, *BMJ*, 2004, **329**, 158-160.
4. J. Rnjak, Z. Li, P. K. Maitz, S. G. Wise and A. S. Weiss, *Biomaterials*, 2009, **30**, 6469-6477.
5. N. O. Ojeh, J. D. Frame and H. A. Navsaria, *Tissue Eng*, 2001, **7**, 457-472.
6. M. Kempf, Y. Miyamura, P. Y. Liu, A. C. Chen, H. Nakamura, H. Shimizu, Y. Tabata, R. M. Kimble and J. R. McMillan, *Biomaterials*, 2011, **32**, 4782-4792.
7. T. Lou, M. Leung, X. J. Wang, J. Y. F. Chang, C. T. Tsao, J. G. C. Sham, D. Edmondson and M. Q. Zhang, *J Biomed Nanotechnol*, 2014, **10**, 1105-1113.
8. S. P. Zhong, Y. Z. Zhang and C. T. Lim, *Wiley Interdiscip Rev Nanomed Nanobiotechnol*, 2010, **2**, 510-525.
9. N. C. Hunt, R. M. Shelton and L. Grover, *Biotechnol J*, 2009, **4**, 730-737.
10. V. M. Schoop, N. Mirancea and N. E. Fusenig, *J Invest Dermatol*, 1999, **112**, 343-353.
11. J. Rnjak-Kovacina, S. G. Wise, Z. Li, P. K. Maitz, C. J. Young, Y. Wang and A. S. Weiss, *Biomaterials*, 2011, **32**, 6729-6736.
12. S. R. Pajoum Shariati, M. A. Shokrgozar, M. Vossoughi and A. Eslamifar, *Iran Biomed J*, 2009, **13**, 169-177.
13. K. J. Doane, W. H. Ting, J. S. McLaughlin and D. E. Birk, *Exp Eye Res*, 1996, **62**, 271-283.
14. R. V. Shevchenko, S. L. James and S. E. James, *J R Soc Interface*, **7**, 229-258.
15. M. P. Curran and G. L. Plosker, *BioDrugs*, 2002, **16**, 439-455.
16. L. Zaulyanov and R. S. Kirsner, *Clin Interv Aging*, 2007, **2**, 93-98.
17. J. Still, P. Glat, P. Silverstein, J. Griswold and D. Mozingo, *Burns*, 2003, **29**, 837-841.
18. H. M. Powell, D. M. Supp and S. T. Boyce, *Biomaterials*, 2008, **29**, 834-843.
19. A. D. Metcalfe and M. W. Ferguson, *J R Soc Interface*, 2007, **4**, 413-437.
20. M. Rinaudo, *Polym. Int.*, 2008, **57**, 397-430.
21. M. P. Lutolf and J. A. Hubbell, *Nature Biotechnology*, 2005, **23**, 47-55.
22. Z. Li, H. R. Ramay, K. D. Hauch, D. Xiao and M. Zhang, *Biomaterials*, 2005, **26**, 3919-3928.
23. Z. Li, M. Leung, R. Hopper, R. Ellenbogen and M. Zhang, *Biomaterials*, 2009, **31**, 404-412.

24. Z. Li and M. Zhang, *Journal of Biomedical Materials Research*, 2005, **75A**, 485-493.
25. N. Bhattarai, D. Edmondson, O. Veiseh, F. A. Matsen and M. Zhang, *Biomaterials*, 2005, **26**, 6176-6184.
26. I.-Y. Kim, S.-J. Seo, H.-S. Moon, M.-K. Yoo, I.-Y. Park, B.-C. Kim and C.-S. Cho, *Biotechnol Adv*, 2008, **26**, 1-21.
27. R. Jayakumar, M. Prabaharan, S. V. Nair and H. Tamura, *Biotechnol Adv*, 2010, **28**, 142-150.
28. K. Y. Lee, L. Jeong, Y. O. Kang, S. J. Lee and W. H. Park, *Adv Drug Deliv Rev*, 2009, **61**, 1020-1032.
29. Chen SH, Tsao CT, Chang CH, Lai YT, Wu MF, Chuang CN, Chou HC, Wang CK and H. KH., *Mater Sci Eng C Mater Biol Appl*, 2013, **33**, 2584-2594.
30. N. Bhattarai, H. R. Ramay, J. Gunn, F. A. Matsen and M. Zhang, *J Control Release*, 2005, **103**, 609-624.
31. N. Bhattarai, F. A. Matsen and M. Zhang, *Macromol Biosci*, 2005, **5**, 107-111.
32. R. A. Clark, *J Invest Dermatol*, 1990, **94**, 128S-134S.
33. K. W. M. S. N. Coolen, E. Middelkoop, M. W. Ulrich, *Arch Dermatol Res*, 2010, **302**, 47-55.
34. M. C. Heng, *Int J Dermatol*, 2011, **50**, 1058-1066.
35. Z. Qiu, A. H. Kwon and Y. Kamiyama, *J Surg Res*, 2007, **138**, 64-70.
36. S. Werner, T. Krieg and H. Smola, *J Invest Dermatol*, 2007, **127**, 998-1008.
37. M. M. Vaidya and D. Kanojia, *J Biosci*, 2007, **32**, 629-634.
38. H. Torma, *Dermatoendocrinol*, 2011, **3**, 136-140.
39. H. Alam, L. Sehgal, S. T. Kundu, S. N. Dalal and M. M. Vaidya, *Mol Biol Cell*, 2011, **22**, 4068-4078.
40. X. Fu, X. Sun, X. Li and Z. Sheng, *Lancet*, 2001, **358**, 1067-1068.
41. J. Attia, N. Bigot, D. Goux, Q. T. Nguyen, K. Boumediene and J. P. Pujol, *J. Bioact. Compat. Pol.*, 2011, **26**, 71-88
42. M. M. Vaidya and D. Kanojia, *J. Biosci.*, 2007, **32**, 629-634.
43. R. K. Schneider, J. Anraths, R. Kramann, J. Bornemann, M. Bovi, R. Knuchel and S. Neuss, *Biomaterials*, 2010, **31**, 7948-7959.
44. L. Weber, E. Kirsch, P. Muller and T. Krieg, *J. Invest. Dermatol.*, 1984, **82**, 156-160.
45. C. N. Metz, *Cell Mol. Life Sci.*, 2003, **60**, 1342-1350.
46. N. Coolen, K. W. M. Schouten, E. Middelkoop and M. W. Ulrich, *Arch. Dermatol. Res.*, 2010, **302**, 47-55.
47. K. A. Bielefeld, S. Amini-Nik, H. Whetstone, R. Poon, A. Youn, J. Wang and B. A.

574 Alman, *J. Biol. Chem.*, 2011, **286**, 27687-27697.
575 48. A. B. Hilmi, A. S. Halim, A. Hassan, C. K. Lim, K. Noorsal and I. Zainol, *Springerplus*,
576 2013, **2**, 79-87.
577 49. R. A. Bader, K. T. Herzog and W. J. Kao, *Polym Bull*, 2009, **62**, 381-389.
578 50. D. Nowinski, P. Hoijer, T. Engstrand, K. Rubin, B. Gerdin and M. Ivarsson, *J Invest*
579 *Dermatol*, 2002, **119**, 449-455.
580 51. M. Prunieras, M. Regnier and D. Woodley, *J Invest Dermatol*, 1983, **81**, 28s-33s.
581 52. J. Attia, K. Boumédiène, J. P. Pujol, J. M. Valleton, E. Huet and Q. T. Nguyen, *J. Bioact.*
582 *Compat. Pol.*, 2009, **24**, 329-349.
583 53. J Attia, Nicolas Bigot, Didier Goux, Quang Trong Nguyen, K. Boumediene and J. P.
584 Pujol, *J Bioact Compat Pol*, 2011, **26**, 71-88
585 54. N. Bhattarai, H. R. Ramay, J. Gunn, F. A. Matsen and M. Zhang, *J. Control. Release*,
586 2005, **103**, 609-624.
587 55. N. Bhattarai, F. A. Matsen and M. Zhang, *Macromol. Biosci.*, 2005, **5**, 107-111.
588 56. Z. Li and M. Zhang, *J. Biomed. Mater. Res.*, 2005, **75A**, 485-493.
589
590
591